Chapter 2
Encounters in Space

Abstract Astronomical observations of the asteroid belt, size distribution and frequency of Earth-crossing asteroids (Apollo and Aten class asteroids) are consistent with the impact history of Earth as progressively revealed by geological and geophysical studies.

Asteroids constitute stony aggregates formed by initial accretion of dust and stony particles, as well as fragmentation associated with subsequent collisions. Nearly two million bodies form the asteroid belt, located between Jupiter and Mars at 2.15–3.3 AU (255–600 million km). These bodies constitute remnants of the original formation of the solar system. Over 50 % of the asteroid belt's mass consists of the large asteroids—*Ceres* (950 km), *Vesta* (530 km) (Fig. 2.1), *Pallas* (530–565 km) and *Hygiea* (350–500 km). More than 200 asteroids measure over 100 km in diameter and 700,000 to 1,700,000 asteroids exceed 1 km in size, the rest ranging down to dust particles. Comets, rich in dust and ice, on short-lived elliptical trajectories, arrive from the Oort Cloud on the fringes of the Solar system, travelling at about half the speed of asteroids (~25–30 km s^{-1}). Whereas comets retain solid cratered surfaces they release tails of vapor representing melting of ice, as on comet Wilde-2 (Fig. 2.2). Periodic collisions between these bodies send fragments hurtling toward Jupiter which, thanks to its huge gravity pull (24.79 m/s^2, as compared with the Earth's 9.78 m/s^2), sweeps up most of these fragments, as observed by the renowned Shoemaker-Levy-9 comet impact (Fig. 2.3), thus protecting the Earth from an extraterrestrial flux which could have arrested the development of advanced life. In an uncanny juxtaposition between mythology and science, the Romans viewed the god *Jupiter* as protector of the State.

Asteroids include the main types (NASA 2012):

1. Carbonaceous (C-type) asteroids are depleted in hydrogen and helium, have chemical ratios akin to solar composition, have low albedo (0.03–0.09), include more than 75 % of known asteroids and inhabit the main belt's outer regions;
2. Siliceous (S-type) asteroids consist of metallic iron mixed with iron- and magnesium-silicates, show high albedo of 0.10–0.22, include about 17 % of known asteroids and occupy the inner asteroid belt. S-type asteroids display various degrees of melting and segregation of metal from silicate.

A. Y. Glikson, *The Asteroid Impact Connection of Planetary Evolution*, SpringerBriefs in Earth Sciences, DOI: 10.1007/978-94-007-6328-9_2,

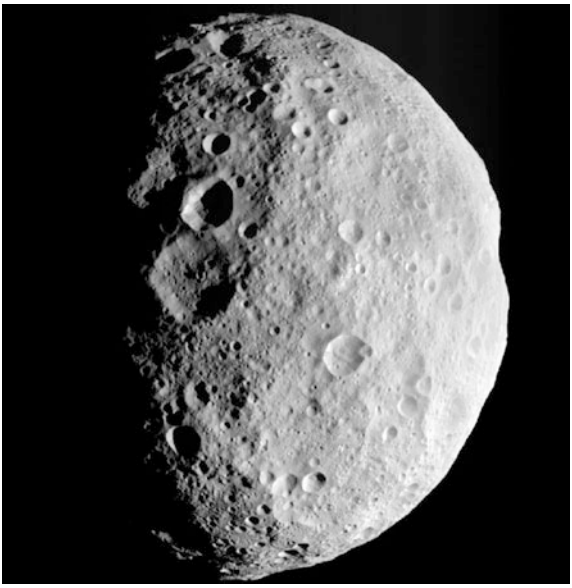

Fig. 2.1 The Dawn spacecraft last view of asteroid 4-Vesta's North Pole, viewed from NASA's Dawn spacecraft. http://www.space.com/17461-dawn-spacecraft-leaves-giant-asteroid-vesta.html. 4-Vesta, with a diameter of 525 km, is the second largest asteroid after Ceres (952 km) (Table 2.1) and forms about 9 % of the mass of the asteroid belt. Vesta lost about 1 % of its mass in a collision, with debris from this event represented by howardite–eucrite–diogenite (HED) meteorites. The Dawn spacecraft entered an orbit around Vesta on 16 July 2011 for a one-year exploration. (NASA)

3. Metallic (M-type) asteroids consist of metallic iron, display high albedo (0.10–0.18) and inhabit the middle part of the asteroid belt.

The total mass of asteroids would form a body of ~1,500 km diameter and 16 asteroids are of diameters 240 km or larger, as in Table 2.1. Asteroid orbits are elliptical rotating in the same direction as the Earth taking over 3–6 years to complete a full course around the Sun. Near Earth asteroids (NEA) at orbits of about 1.3 AU (~195.10^6 km) include the following categories: (a) *Amor* class asteroids cross the Mars orbit, the typical one being *Eros*; (b) *Apollo* class asteroids cross Earth's orbit with a period greater than 1 year, an example being *Geographos*; (c) *Aten* class asteroids cross Earth's orbit with a period less than 1 year, an example being *Ra-Shalom*. NEA whose orbits lie between 0.983 and 1.3 astronomical units (AU) away from the Sun pose a potential impact risk for Earth. By 2012 the number of NEA detected by NASA reached 9,252 near Earth asteroids (NEA) of which ~2,250 objects are of diameters ~100–300 m, ~2,800 objects of diameters 300–1,000 m and 850 objects of diameters >1 km (NASA 2012).

An earlier explanation of the origin of the asteroid belt has been advanced in terms of the breakdown of a planet smaller than Earth. The modern view is based

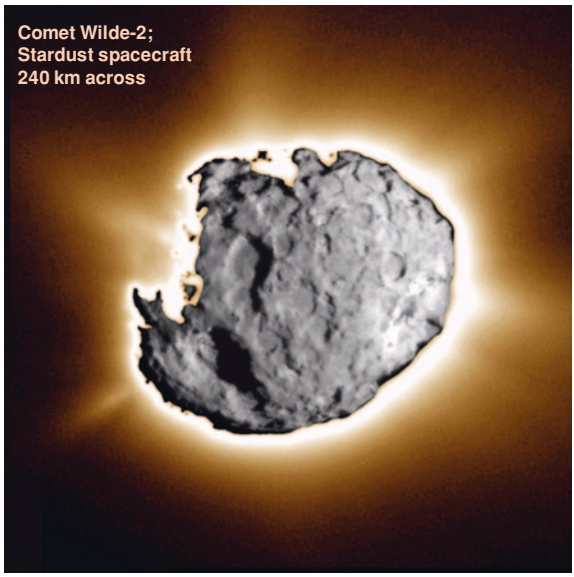

Fig. 2.2 Comet Wild-2 of 5 km diameter http://ucsdnews.ucsd.edu/newsrel/science/mcstardust.asp. An image taken from the spacecraft Stardust on the 2 January, 2004. As the spacecraft flew through this material, a special collection grid filled with aerogel-b, a novel sponge-like material that's more than 99 % empty space, gently captured samples of the comet's gas and dust. The grid was stowed in a capsule which detached from the spacecraft and parachuted to Earth on 15 January, 2006. Since then, scientists around the world have been busy analyzing the samples to learn the secrets of comet formation and our solar system's history. The samples contained Glycine, an amino acid used by living organisms to make proteins, and this is the first time an amino acid has been found in a comet. http://stardust.jpl.nasa.gov/news/news115.html. (NASA)

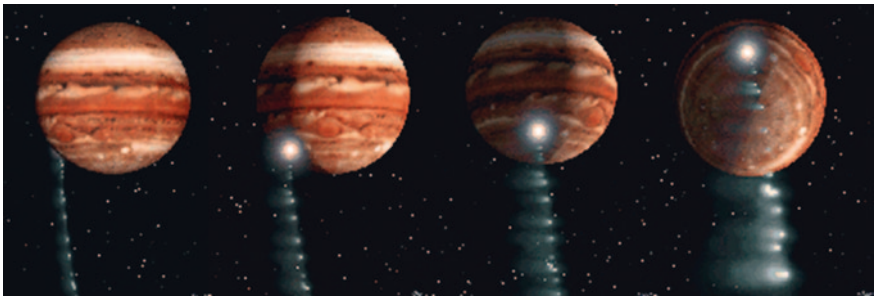

Fig. 2.3 The collision of 21 fragments (with diameters of up to 2 km) of the Comet Shoemaker-Levy-9 with Jupiter on 16 July, 1994, projected in advance by David Levy, Caroline Shoemaker and Eugene Shoemaker, constituted the first directly observed extraterrestrial collision in the solar system. It was photographed with a 40 cm Schmidt telescope at the Palomar Observatory in California. The fragmented nature of the comet is attributed to a previous approach to Jupiter in July 1992 within the Roche fragmentation limit. Impact speed is measured as 60 km/s http://www2.jpl.nasa.gov/sl9/. (NASA)

Table 2.1 Approximate number of asteroids N close to diameter D

D	N	Examples
100 m	~25,000,000	2011 AG5 (D ~ 140 m)
300 m	4,000,000	Apophis (D ~ 270 m)
500 m	2,000,000	2005 YU55 (D ~ 400 m)
1 km	750,000	1998 SF36 (D ~ 725 m)
3 km	200,000	Toutatis (D ~ 2.3–5.3 km)
5 km	90,000	Otawara (D ~ 5.5 km)
10 km	10,000	Gaspra (D ~ 19 × 12 × 11)
30 km	1,100	Eros (D ~ 34 × 11 × 11 km)
50 km	600	Ida (D ~ 58 × 23 km)
100 km	200	Lutetia (D ~ 100 km)
200 km	30	Iris (D ~ 213 km)
300 km	5	Interamnia (D ~ 326 km)
500 km	3	Vesta (D ~ 525 km); Pallas (D ~ 545 km); Hygiea (D ~ 431 km)
900 km	1	Ceres (D ~ 952 km)

on the compositional diversity of asteroids, suggesting the asteroid belt formed during the first 10 million years of solar history through gravitational accretion from the primitive solar disc, followed by aggregation, limited melting and fractionation. After their formation, the asteroids underwent an early stage of internal heating and surface melting due to impacts and surface erosion by the solar wind and micrometeorites. The NEAR Shoemaker mission, aimed at observing *Eros* (preface photograph), its surface features, chemistry, mineral composition, spin state, magnetic field and the effects of the solar wind. The probe carried 56 kg of equipment, including an X-ray/gamma ray spectrometer, a near-infrared spectrograph, a multispectral camera, a laser range finder and a magnetometer. *Eros* is an S-type asteroid, namely a body dominated by silicate minerals. NEAR Shoemaker's other task was to draw comparisons between the composition of this asteroid and S-Type meteorites found on Earth. The mission ended with a touchdown in the "saddle" region of *Eros*. Although NEAR Shoemaker was not designed as a Lander, the craft's gamma-ray spectrometer continued to collect data for 2 weeks on the elemental composition of *Eros*. The spacecraft made its last call to Earth on 28 February 2001.

Several space encounters with asteroids and comets followed. The Japanese *Hayabusa* probe collected asteroid debris from the asteroid *Itokawa* (640 × 270 m) on 12 September 2005. NASA's Deep Impact probe encountered the cratered nucleus of comet *Tempel-1* (100–200 m.) on 4 July 2005. On 10 July this year, the European Space Agency's probe *Rosetta* passed 3,162 km from the asteroid *Lutetia* (long axis 134 km) at a speed of 15 km/s. *Rosetta's OSIRIS* images of *Lutetia*, taken with both wide-angle and narrow-angle cameras, with resolution to 60 m, show large, eroded craters imprinted by young, well-defined craters. *Lutetia* shows spectral characteristics intermediate between those of C-Type asteroids and M-Type asteroids.

In the wake of the Late Heavy Bombardment during ~3.95–3.85 Ga impacts by very large asteroids and comets in the inner solar system declined from

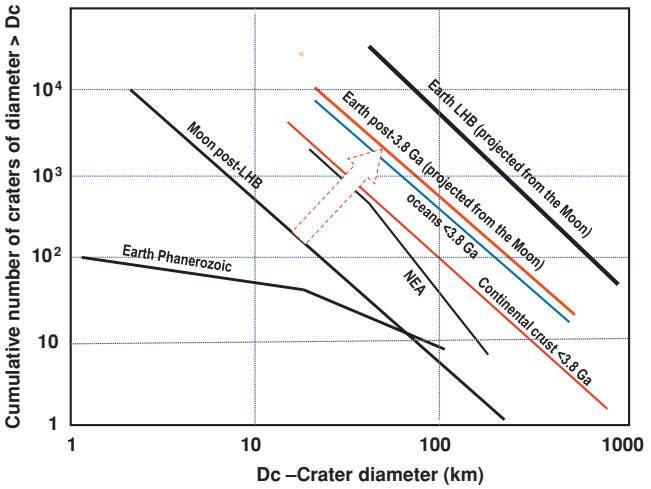

Fig. 2.4 Crater diameter versus cumulative number of craters of diameters <Dc for (1) Late heavy bombardment of Earth, extrapolated from lunar data of Barlow (1990); (2) Lunar post-Late Heavy Bombardment (*LHB*); (3) Earth post 3.8 Ga (projected from the Moon); (4) Earth oceans (~80 % of the Earth's surface); Earth continental crust (~20 % of the Earth surface); (5) Phanerozoic impact rates displaying erosional loss of small craters (modified after Grieve and Dence 1979)

a flux of $4–9 \cdot 10^{-13}$ km^2 year^{-1} (for craters Dc $\geq$ 18 km) to a flux of $3.8–6.3 \cdot 10^{-15}$ km^2 year^{-1} (for craters Dc $\geq$ 20 km) (Grieve and Dence 1979; Baldwin 1985; Ryder 1990). Post-LHB impact rates on Earth estimated from lunar crater counts on Mare surfaces are of the same order of magnitude as cratering rate of $5.9 \pm 3.5.10^{-15}$ km^{-2} year^{-1} (for craters Dc $\geq$ 20 km), as estimated from astronomical observations of near-Earth asteroids (NEA) and comets (Shoemaker and Shoemaker 1996). These authors estimated an impact flux where N ∞ Dc$^{-1.8}$ to N ∞ Dc$^{-2.0}$ (N = cumulative number of craters with diameters larger than Dc; Dc = crater diameter). Plots of crater size versus cumulative crater size frequency as projected from the Moon allow estimates of impact incidence including >100 craters of Dc $\geq$ 300 km and >50 craters of Dc $\geq$ 500 km since the LHB (Fig. 2.4).

To date a minimum of 20 impacts by asteroids >10 km in diameter has been recorded from microkrystite spherule units [~3,482, 3,472–3,467 (2), 3,445, 3,416, 3,334, 3,256, 3,243, 3,225 (2), 2.63, 2.57, 2.56 (2), 2.54, 2.48 Ga] and from large impact structures (2.975 Ga (Maniitsoq—Garde et al. 2012), 2.023 (Vredefort—Gibson and Reimold 2001), 1.85 Ga (Sudbury—Therriault et al. 2002) (Tables 1.1 and 1.2). This implies that about one third of the large asteroid influx estimated from the lunar flux (>100 craters of Dc $\geq$ 300 km, Fig. 2.4) has been identified on Earth to date (Chap. 9). These estimates do not take into account probable and possible as yet unproven impact structures such as the Warburton shock metamorphic terrain (see Sect. 11.6). Such a surprising high rate of preservation is explained by the crustal depth of major impact craters and rebound domes and the relatively high thickness of their ejecta units.

References

Baldwin RB (1985) Relative and absolute ages of individual craters and the rates of infalls on the Moon in the post-imbrium period. Icarus 61:63–91

Barlow NG (1990) Estimating the terrestrial crater production rate during the late heavy bombardment period. Lunar Planet Instit Contrib 746:4–7

Garde AA, McDonald I, Dyck B, Keulen N (2012) Searching for giant ancient impact structures on Earth: the Meso-Archaean Maniitsoq structure, West Greenland. Earth Planet Sci Lett 2012:337–338

Gibson RL, Reimold WU (2001) The vredefort impact structure South Africa: the scientific evidence and a two-day excursion guide. Council Geosci Mem 92:111

Grieve RAF, Dence MR (1979) The terrestrial cratering record: II the crater production rate. Icarus 38:230–242

NASA (2012) Near Earth Objects Program. http://neo.jpl.nasa.gov/stats/, http://nssdc.gsfc.nasa.gov/planetary/text/asteroids.txt

Ryder G (1990) Lunar samples lunar accretion and the early bombardment of the Moon. Eos (Trans Am Geophys Union) 71:313–322

Shoemaker EM, Shoemaker CS (1996) The proterozoic impact record of Australia. Aust Geol Surv Org J Aust Geol Geophys 16:379–398

Therriault AM, Anthony D, Flower R, Grieve RAF (2002) The sudbury igneous complex: a differentiated impact melt sheet. Econ Geol 97:1521–1540

http://www.springer.com/978-94-007-6327-2

The Asteroid Impact Connection of Planetary Evolution
With Special Reference to Large Precambrian and Australian impacts

Glikson, A.Y.

2013, XII, 149 p. 54 illus., 46 illus. in color., Softcover
ISBN: 978-94-007-6327-2